A NONCONFORMING IMMERSED VIRTUAL ELEMENT METHOD FOR ELLIPTIC INTERFACE PROBLEMS

HYEOKJOO PARK AND DO Y. KWAK

Abstract. This paper presents the lowest-order nonconforming immersed virtual element method for solving elliptic interface problems on unfitted polygonal meshes. The local discrete space on each interface mesh element consists of the solutions of local interface problems with Neumann boundary conditions, and the elliptic projection is modified so that its range is the space of broken linear polynomials satisfying the interface conditions. We derive optimal error estimates in the broken H^1-norm and L^2-norm, under the piecewise H^2-regulartiy assumption. In our scheme, the mesh assumptions for error analysis allow small cut elements. Several numerical experiments are provided to confirm the theoretical results.

1. Introduction

In recent years, there has been a lot of interest in developing numerical methods for solving partial differential equations (PDEs) on general polygonal/polyhedral meshes, including mimetic finite difference (MFD) methods [12,19,21], hybrid high-order (HHO) methods [31,36], hybridizable discontinuous Galerkin (HDG) methods [33,34], weak Galerkin (WG) methods [59,65], and so on. Among them, the virtual element method (VEM), as an evolution of the MFD method into the framework of the finite element method (FEM), was introduced in [7]. The main feature of the VEM is that the local shape functions, called the virtual elements, are defined implicitly as the solutions of certain local PDEs, and they are characterized by the degrees of freedom (DOFs). Although it is impossible to construct these functions explicitly in general, the VEM can be implemented using the DOFs only. The VEM also has been successfully developed for a wide range of problems: Stokes problem [13,24], elasticity problem [9,51,66], Maxwell problem [8,11], etc. We also refer to [2,5,10,20,49] and the references therein for more thorough survey.

On the other hand, there are numerous engineering and physical problems where the underlying PDEs have an interface, such as multiphase flows, solid mechanics with multiple materials, and Hele-Shaw flows, etc (see, e.g., [6, 40, 42, 47]). The PDEs governing such problems involve with discontinuous coefficients across the interface, which usually leads to low global regularity of the solution, even when the interface is smooth. The low global regularity causes a deterioration in performance of the traditional FEMs, unless the mesh is aligned with the interface. However, it takes a lot of time to generate interface-fitted meshes when the interface is geometrically complicated or is moving as time evolves. For such cases, it may be more

2020 *Mathematics Subject Classification.* 65N12, 65N15, 65N30.

Key words and phrases. immersed virtual element method, nonconforming method, elliptic interface problem, unfitted mesh, polygonal mesh.

This work is partially supported by NRF, contract No. 2021R1A2C1003340.

efficient to use unfitted or structured meshes than fitted meshes. Moreover, one can exploit geometric multigrid methods for the structured meshes. Researchers developed several numerical schemes using unfitted triangular or rectangular meshes: cut FEMs [39, 40], extended FEMs [14, 15], and immersed FEMs [52, 56, 57], to name just a few. In particular, the immersed FEM modifies the traditional finite elements so that they satisfy the interface conditions, while keeping the optimal approximation capabilities. Lagrange-type elements were studied in [41, 56, 57], while nonconforming-type elements were studied in [44, 52, 58]. Other related works can be found in [27, 38, 43, 45, 48, 50, 53] and the references therein.

Due to the great flexibility of polygonal meshes in the mesh generation process, several researchers focused on developing interface-fitted polygonal mesh generators and analyzing schemes for interface problems on such meshes (see, e.g., [28, 60, 64]). Nevertheless, it would be still attractive to use unfitted polygonal meshes in some situations, such as problems involving moving interfaces as time evolves or during the computation of the free-boundary problems. Recently, several numerical schemes using unfitted polygonal meshes were developed. The authors in [22, 23] proposed the unfitted HHO method for elliptic interface problems, where a Nitsche-type formulation is used. They proved that the method exhibits an optimal error estimate in the H^1-norm. However, to ensure the optimal convergence, it requires some additional mesh procedures, which prevent the appearance of small cut elements. The lowest-order Lagrange-type immersed VEM for triangular meshes was developed in [26]. Unlike the Lagrange-type immersed FEM, the local shape functions are conforming, and DG-type consistency terms are not required to guarantee the optimal convergence. However, its convergence analysis is limited to the triangular meshes. The virtual finite element method [25] was also developed for solving two-dimensional Maxwell interface problems, in which each interface element is divided into subtriangles and the local space on the interface element is defined by piecewise Nédélec elements. However, its convergence analysis is also limited to the triangular meshes. The immersed WG method on triangular meshes was proposed in [61], and extended to polygonal meshes in [62]. Compared to the lowest-order unfitted HHO method, the immersed WG method requires less restrictive mesh assumptions: the unfitted HHO method requires that two subregions of each interface element divided by the interface must contain a ball with radius comparable to the diameter of the element, while the immersed WG does not require such conditions. However, the immersed WG requires an additional regularity assumption: The Darcy velocity must be H^1 on the entire domain.

In this paper, we define and analyze the lowest-order nonconforming immersed VEM for elliptic interface problems on unfitted polygonal meshes. Motivated by the conforming immersed VEM [26] and the nonconforming VEM [5], we define the virtual elements on each interface mesh element by the solutions of local interface problems with Neumann boundary conditions, and the elliptic projection is modified so that its range is the space of broken linear polynomials satisfying interface conditions, which is also used in the linear immersed FEMs (see, e.g., [52, 56]). We derive optimal error estimates in the broken H^1-norm and L^2-norm under the standard regularity assumption that the solution is a piecewise H^2-function. Moreover, as in the immersed WG [62], the mesh assumptions in our scheme allow small cut elements. In addition, since our scheme is also a nonconforming method, the Darcy velocity can be recovered efficiently by casting a mixed formulation into

the nonconforming method (see, e.g., [3, 4, 47, 49, 52]). We also note that, since there is an equivalence relation between the nonconforming VEM and the HHO method [32, 54], we can reformulate our scheme in the context of HHO methods. However, it will be different from the unfitted HHO methods in [22, 23], since these methods use the Nitsche-type formulation, while our method does not.

The rest of the paper is organized as follows. In Section 2, we introduce the model problem and mesh assumptions. In Section 3, we explain the nonconforming immersed VEM. In Section 4, we prove some approximation properties of the discrete spaces. In Section 5, we prove optimal error estimates of our scheme in the broken H^1-norm and the L^2-norm. Finally, we report several numerical tests that confirm the theoretical results in Section 6.

2. Preliminaries

We follow the standard notation of Sobolev spaces (see, e.g., [17, 30]). For an integer $k \geq 0$ and a subset D of $\mathbb{R}$ or $\mathbb{R}^2$, we denote by $\mathbb{P}_k(D)$ the space of all polynomials of degree at most k on D. For a subset A of $\mathbb{R}$ or $\mathbb{R}^2$, the indicator function on A is denoted by χ_A. For a bounded measurable subset D of $\mathbb{R}$ or $\mathbb{R}^2$ and $v \in L^1(D)$, we denote by $(v)_D$ the average of v on D.

2.1. **Model problem.** Let Ω be a polygonal domain in $\mathbb{R}^2$, which is separated into two disjoint subdomains Ω^+ and Ω^- by an interface $\Gamma = \partial\Omega^- \cap \partial\Omega^+$ (see, e.g., Figure 1). Here we assume that Γ is a C^2-curve that is not self-intersecting. For any domain $D \subset \Omega$ and any function $u : D \to \mathbb{R}$, we define its jump across the portion of the interface $\Gamma \cap D$ as

$$[u]_{\Gamma\cap D} := u|_{D\cap\Omega^+} - u|_{D\cap\Omega^-}.$$

We consider the elliptic interface problem: Given $f \in L^2(\Omega)$, find $u \in H_0^1(\Omega)$ such that

$$\begin{cases} -\nabla\cdot(\beta\nabla u) = f & \text{in } \Omega^+\cup\Omega^-, \\ u = 0 & \text{on } \partial\Omega, \end{cases} \tag{2.1}$$

with the jump conditions on the interface

$$[u]_\Gamma = 0, \quad \left[\beta\frac{\partial u}{\partial \boldsymbol{n}}\right]_\Gamma = 0, \tag{2.2}$$

where the coefficient β is positive and piecewise constant on $\Omega^\pm$, that is, $\beta^s := \beta|_{\Omega^s}$ is constant for $s = +, -$. Let $\beta_* = \min\{\beta^+, \beta^-\}$ and $\beta^* = \max\{\beta^+, \beta^-\}$. A weak formulation of the model problem (2.1)-(2.2) is written as follows: Find $u \in H_0^1(\Omega)$ such that

$$(\beta\nabla u, \nabla v)_{0,\Omega} = (f, v)_{0,\Omega} \quad \forall v \in H_0^1(\Omega). \tag{2.3}$$

For any domain $D \subset \Omega$, let us introduce the space

$$\widetilde{H}^2(D) := \left\{u \in H^1(D) : u|_{D\cap\Omega^s} \in H^2(D\cap\Omega^s),\ s = +, -\right\}$$

equipped with the following norm:

$$\|u\|_{2,D^\pm}^2 := \|u\|_{1,D}^2 + |u|_{2,D\cap\Omega^+}^2 + |u|_{2,D\cap\Omega^-}^2.$$

We also define

$$\widetilde{H}_\Gamma^2(D) := \left\{u \in \widetilde{H}^2(D) : [\beta\partial u/\partial\boldsymbol{n}]_{\Gamma\cap D} = 0\right\}.$$

Then we have the following regularity theorem for the problem (2.3); see [16, 29].

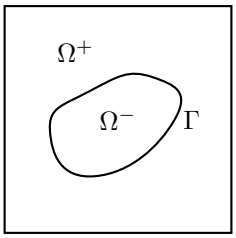

FIGURE 1. A domain Ω with interface Γ.

Theorem 2.1. *Suppose that Ω is a convex polygon in $\mathbb{R}^2$ and $f \in L^2(\Omega)$. Then the problem (2.3) has a unique solution $u \in H_0^1(\Omega) \cap \widetilde{H}_\Gamma^2(\Omega)$ satisfying*

$$\|u\|_{2,\Omega^\pm} \leq C_\Omega \|f\|_{0,\Omega} \tag{2.4}$$

for some generic positive constant C_Ω.

2.2. **Mesh assumptions.** Let $\mathcal{P}_h$ be a decomposition (mesh) of Ω into polygonal elements K with maximum diameter h. Let $\mathcal{E}_h$ be the set of all edges in $\mathcal{P}_h$. Let $\mathcal{E}_h^\circ$ and $\mathcal{E}_h^\partial$ denote the set of all interior and boundary edges in $\mathcal{P}_h$, respectively. For each $K \in \mathcal{P}_h$, let h_K and $|K|$ be the diameter and the area of K, respectively. For each $e \in \mathcal{E}_h$, we denote by $|e|$ the length of e.

An element $K \in \mathcal{P}_h$ is called an interface element if the interface Γ passes through the interior of K; otherwise K is called a non-interface element. We denote by $\mathcal{P}_h^I$ and $\mathcal{P}_h^N$ the collections of all interface and non-interface elements in $\mathcal{P}_h$, respectively. Analogously, an edge $e \in \mathcal{E}_h$ is called an interface edge if Γ passes through the interior of e; otherwise e is called a non-interface edge. The collection of all interface edges and non-interface edges in $\mathcal{E}_h$ are denoted by $\mathcal{E}_h^I$ and $\mathcal{E}_h^N$, respectively. For each $K \in \mathcal{P}_h$, let $\mathcal{E}_K^I$ and $\mathcal{E}_K^N$ be the set of all interface and non-interface edges of K, and let $\mathcal{E}_K := \mathcal{E}_K^I \cup \mathcal{E}_K^N$.

We assume that h is sufficiently small, and $\mathcal{P}_h$ satisfies the following regularity assumptions [5, 7, 20].

Assumption 2.2. There exists $\rho > 0$ independent of h such that

(i) the decomposition $\mathcal{P}_h$ consists of a finite number of nonoverlapping polygonal elements;
(ii) every element $K \in \mathcal{P}_h$ is star-shaped with respect to a ball B_K with center $\boldsymbol{x}_K$ and radius ρh_K;
(iii) for each element $K \in \mathcal{P}_h$, all the edges in K have length larger than ρh_K;
(iv) the interface Γ meets the edges of each interface element at no more than two points;
(v) the interface Γ meets each edge in $\mathcal{E}_h$ at most once, except possibly it passes through two vertices.

Remark that the assumptions (iv) and (v) are reasonable for sufficiently small h. As mentioned earlier, these assumptions allow small cut elements and do not require additional mesh procedures.

For each $K \in \mathcal{P}_h$, let $\boldsymbol{n}_K$ be the exterior unit normal vector along ∂K. For each $e \in \mathcal{E}_h$, let $\boldsymbol{n}_e$ be a unit normal vector of e with orientation fixed once and for all. Let $e \in \mathcal{E}_h^\circ$ and let K_1 and K_2 be the polygons in $\mathcal{P}_h$ having e as a common edge.

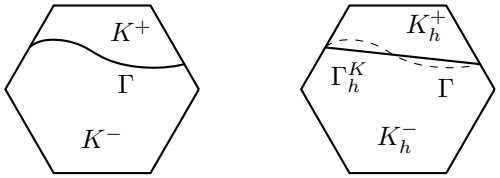

FIGURE 2. An interface element K in $\mathcal{P}_h$.

For $u : \Omega \to \mathbb{R}$ satisfying $u|_{K_1} \in H^1(K_1)$ and $u|_{K_2} \in H^1(K_2)$, we define the jump of u on e by

$$[u]_e := (u|_{K_1})(\boldsymbol{n}_{K_1} \cdot \boldsymbol{n}_e) + (u|_{K_2})(\boldsymbol{n}_{K_2} \cdot \boldsymbol{n}_e).$$

For $e \in \mathcal{E}_h^\partial$, we define $[u]_e := u|_e$. We use the notations ∇_h and $\nabla_h \cdot$ when the gradient and divergence operators are taken elementwise for piecewise smooth functions on $\mathcal{P}_h$.

Let $K \in \mathcal{P}_h^I$. For $s = +, -$, we define $K^s := K \cap \Omega^s$. We denote by Γ_h^K the line segment connecting the intersections of Γ and the edges of K. This line segment divides K into two parts K_h^+ and K_h^- with $\overline{K} = \overline{K_h^+ \cup K_h^-}$ (see, e.g., Figure 2). For each $e \in \mathcal{E}_h^I$, we let $e^s := e \cap \Omega^s$ for $s = +, -$. We define the jumps of a function $u : K \to \mathbb{R}$ across $\Gamma_h^K \cap K$ as

$$[u]_{\Gamma_h^K} := u|_{K_h^+} - u|_{K_h^-}.$$

Let β_h be the piecewise constant function on Ω defined as follows:

$$\beta_h|_K := \begin{cases} \beta^+ \chi_{K_h^+} + \beta^- \chi_{K_h^-} & \text{if } K \in \mathcal{P}_h^I, \\ \beta & \text{otherwise.} \end{cases}$$

We also define $\beta_K^* := \|\beta_h\|_{L^\infty(K)}$. Let $\Gamma_h = \bigcup_{K \in \mathcal{P}_h^I} \Gamma_h^K$, and let $\boldsymbol{n}_\Gamma^h$ and $\boldsymbol{t}_\Gamma^h$ be the unit normal and tangential vectors along Γ_h.

3. Nonconforming immersed virtual element method

In this section, we present the nonconforming immersed virtual element method for the elliptic interface problem (2.3).

3.1. Broken linear polynomials.

We consider the space of piecewise linear polynomials satisfying the interface conditions on each interface element. Let $K \in \mathcal{P}_h$ be an interface element. The broken polynomial space $\widehat{\mathbb{P}}_1(K)$ is defined by

$$\widehat{\mathbb{P}}_1(K) := \left\{ q \in H^1(K) : q|_{K_h^s} \in \mathbb{P}_1(K_h^s) \ \forall s = +, -, \ [\beta_h \partial q / \partial \boldsymbol{n}]_{\Gamma_h^K} = 0 \right\}.$$

It is easy to see that $\dim \widehat{\mathbb{P}}_1(K) = 3$ and the following piecewise polynomials form a basis of $\widehat{\mathbb{P}}_1(K)$:

$$q_1(\boldsymbol{x}) = 1, \quad q_2(\boldsymbol{x}) = \boldsymbol{t} \cdot (\boldsymbol{x} - \boldsymbol{x}_0), \quad q_3(\boldsymbol{x}) = \beta_h^{-1} \boldsymbol{n} \cdot (\boldsymbol{x} - \boldsymbol{x}_0),$$

where $\boldsymbol{x}_0$ is the midpoint of the line segment Γ_h^K, $\boldsymbol{n} = (n_1, n_2)$ is a unit vector normal to Γ_h^K pointing from K_h^+ to K_h^-, and $\boldsymbol{t} = (-n_2, n_1)$. Since $\widehat{\mathbb{P}}_1(K) \subset H^1(K)$, the space $\nabla \widehat{\mathbb{P}}_1(K)$ is well-defined, and ∇q_2 and ∇q_3 form a basis of $\nabla \widehat{\mathbb{P}}_1(K)$.

We set $\widehat{\mathbb{P}}_1(K) := \mathbb{P}_1(K)$ for non-interface element $K \in \mathcal{P}_h$.

3.2. **Nonconforming immersed virtual elements.** We first define the local space on each element. For each interface element $K \in \mathcal{P}_h$, let

$$V_h(K) := \Big\{ v \in H^1(K) : \nabla \cdot \beta_h \nabla v = 0 \text{ in } K,\ \beta_h \partial v/\partial \boldsymbol{n} \in \widetilde{\mathbb{P}}_0(e)\ \forall e \in \mathcal{E}_K, \\ [\beta_h \partial v/\partial \boldsymbol{n}]_{\Gamma_h^K} = 0 \text{ on } \Gamma_h^K \Big\},$$

where $\widetilde{\mathbb{P}}_0(e)$ is defined by

$$\widetilde{\mathbb{P}}_0(e) := \{ a\chi_{e^+} + b\chi_{e^-} : a, b \in \mathbb{R} \} \quad \text{for } e \in \mathcal{E}_h^I,$$

and $\widetilde{\mathbb{P}}_0(e) := \mathbb{P}_0(e)$ for $e \in \mathcal{E}_h^N$. Proceeding as in Lemma 3.1 in [5], it is easy to verify that $\widehat{\mathbb{P}}_1(K) \subset V_h(K)$ and the DOFs of $V_h(K)$ can be chosen as follows:

$$\tfrac{1}{|e^+|} \textstyle\int_{e^+} v \,\mathrm{d}s, \quad \forall e \subset \partial K \text{ with } e \in \mathcal{E}_h^I, \tag{3.1a}$$

$$\tfrac{1}{|e^-|} \textstyle\int_{e^-} v \,\mathrm{d}s, \quad \forall e \subset \partial K \text{ with } e \in \mathcal{E}_h^I, \tag{3.1b}$$

$$\tfrac{1}{|e|} \textstyle\int_{e} v \,\mathrm{d}s, \quad \forall e \subset \partial K \text{ with } e \in \mathcal{E}_h^N, \tag{3.1c}$$

For each non-interface element $K \in \mathcal{P}_h$, the local space is defined as in the standard nonconforming VEM [5]:

$$V_h(K) := \big\{ v \in H^1(K) : \Delta v = 0 \text{ in } K,\ \partial v/\partial \boldsymbol{n} \in \mathbb{P}_0(e)\ \forall e \in \mathcal{E}_K \big\},$$

and its DOFs can be chosen as (3.1c).

Remark 3.1. If the local space $V_h(K)$ on the interface element K defined as in the local space in the non-interface element, then the inclusion $\widehat{\mathbb{P}}_1(K) \subset V_h(K)$ and the interface condition $[\beta_h \partial v/\partial \boldsymbol{n}]_{\Gamma_h^K} = 0$ does not hold. It may lead difficulties in analysis and extending our scheme to some other applications such as the nonhomogeneous interface problems.

The global nonconforming immersed virtual element space $V_h(\Omega)$ is given by

$$V_h(\Omega) := \Big\{ v_h \in L^2(\Omega) : v_h|_K \in V_h(K) \quad \forall K \in \mathcal{P}_h, \\ \int_e [v_h]_e q \,\mathrm{d}s = 0 \quad \forall q \in \widetilde{\mathbb{P}}_0(e),\ \forall e \in \mathcal{E}_h \Big\}.$$

Note that the DOFs of $V_h(\Omega)$ are the edge moments (3.1) for $e \in \mathcal{E}_h^\circ$.

For $K \in \mathcal{P}_h$ and $v \in H^1(K)$, the local interpolant $I_h^K v$ is defined as the unique element of $V_h(K)$ satisfying

$$\int_e I_h^K v q \,\mathrm{d}s = \int_e v q \,\mathrm{d}s \quad \forall q \in \widetilde{\mathbb{P}}_0(e),\ \forall e \in \mathcal{E}_K.$$

Analogously, for $v \in H_0^1(\Omega)$, the (global) interpolant $I_h v$ is defined as the unique element of $V_h(\Omega)$ such that

$$\int_e I_h v q \,\mathrm{d}s = \int_e v q \,\mathrm{d}s \quad \forall q \in \widetilde{\mathbb{P}}_0(e),\ \forall e \in \mathcal{E}_h.$$

Let $H_h(\Omega) := V_h(\Omega) + H_0^1(\Omega)$. We define the broken H^1-seminorm on $H_h(\Omega)$ by

$$|v_h|_{1,h}^2 = \sum_{K \in \mathcal{P}_h} \|\nabla v_h\|_{0,K}^2, \quad \forall v_h \in H_h(\Omega).$$

3.3. **The discrete problem.** In order to define the discrete bilinear form $a_h(\cdot,\cdot)$ on $H_h(\Omega)$, we first introduce some projection operators on the mesh elements and mesh edges. For each $K \in \mathcal{P}_h$, let Π_K^∇ be the projection from $H^1(K)$ onto $\widehat{\mathbb{P}}_1(K)$ satisfying

$$\int_K \beta_h \nabla \Pi_K^\nabla v \cdot \nabla q \,\mathrm{d}\boldsymbol{x} = \int_K \beta_h \nabla v \cdot \nabla q \,\mathrm{d}\boldsymbol{x} \quad \forall q \in \widehat{\mathbb{P}}_1(K), \tag{3.2}$$

$$\int_{\partial K} \Pi_K^\nabla v \,\mathrm{d}s = \int_{\partial K} v \,\mathrm{d}s. \tag{3.3}$$

Note that integration by parts gives

$$\int_K \beta_h \nabla v \cdot \nabla q \,\mathrm{d}\boldsymbol{x} = \int_{\partial K} \beta_h \nabla q \cdot \boldsymbol{n}_K v \,\mathrm{d}s \quad \forall v \in H^1(K),\ \forall q \in \widehat{\mathbb{P}}_1(K).$$

Here, since $\beta_h \nabla q \cdot \boldsymbol{n}_e \in \widetilde{\mathbb{P}}_0(e)$ on each $e \subset \partial K$, the projection $\Pi_K^\nabla v$ of $v \in V_h(K)$ can be computed by the DOFs of v. For $v \in H_h(\Omega)$, we define $\Pi^\nabla v$ by the piecewise broken linear polynomial such that $(\Pi^\nabla v)|_K = \Pi_K^\nabla(v|_K)$ for any $K \in \mathcal{P}_h$.

Next, for each edge $e \in \mathcal{E}_h$, let Π_e^∂ be the L^2-projection from $L^2(e)$ onto $\widetilde{\mathbb{P}}_0(e)$. For $v \in H^1(K)$ with $K \in \mathcal{P}_h$, let $\Pi_K^\partial v$ be such that $(\Pi_K^\partial v)|_e = \Pi_e^\partial(v|_e)$ for any $e \subset \partial K$. Analogously, for $v \in H_h(\Omega)$, let $\Pi^\partial v$ be such that $(\Pi^\partial v)|_e = \Pi_e^\partial(v|_e)$ for any $e \in \mathcal{E}_h$.

For each $K \in \mathcal{P}_h$, we define

$$a_h^K(u,v) := \left(\beta_h \nabla \Pi_K^\nabla u, \nabla \Pi_K^\nabla v\right)_{0,K} + S_h^K\left(u - \Pi_K^\nabla u, v - \Pi_K^\nabla v\right), \quad u, v \in H^1(K),$$

where S_h^K is the stabilization term defined by

$$S_h^K(u,v) := \frac{\beta_K^*}{h_K}\left(\Pi_K^\partial u, \Pi_K^\partial v\right)_{0,\partial K}, \quad u, v \in H^1(K).$$

The discrete bilinear forms a_h and S_h on $H_h(\Omega)$ are defined by

$$a_h(u_h, v_h) := \sum_{K \in \mathcal{P}_h} a_h^K(u_h, v_h), \quad S_h(u_h, v_h) = \sum_{K \in \mathcal{P}_h} S_h^K(u_h, v_h),$$

We also define the discrete energy norm $|||\cdot|||$ on $H_h(\Omega)$ by $|||v_h|||^2 := a_h(v_h, v_h)$. It is indeed a norm on $V_h(\Omega)$, as given in the following lemma.

Lemma 3.2. *$|||\cdot|||$ is a norm on $V_h(\Omega)$.*

Proof. It is clear that $|||\cdot|||$ is a seminorm. Thus it suffices to show that $v_h = 0$ if $|||v_h||| = 0$ for $v_h \in V_h(\Omega)$. Let $v_h \in V_h(\Omega)$ satisfy $|||v_h||| = 0$. Then we have $\nabla \Pi^\nabla v_h = 0$ and $\Pi^\partial(v_h - \Pi^\nabla v_h) = 0$. Since $v_h \in V_h(\Omega)$, we have

$$\begin{aligned}
\beta_* \|\nabla v_h\|_{0,K}^2 &\le (\beta_h \nabla v_h, \nabla v_h)_{0,K} = (\beta_h \nabla v_h, \nabla(v_h - \Pi_K^\nabla v_h))_{0,K} \\
&= (\beta_h \nabla v_h \cdot \boldsymbol{n}_K, v_h - \Pi_K^\nabla v_h)_{0,\partial K} = (\beta_h \nabla v_h \cdot \boldsymbol{n}_K, \Pi_K^\partial(v_h - \Pi_K^\nabla v_h))_{0,\partial K} \\
&= 0
\end{aligned}$$

for any $K \in \mathcal{P}_h$. Thus v_h is constant on every $K \in \mathcal{P}_h$. Since $\Pi_e^\partial [v_h]_e = 0$ for any edge $e \in \mathcal{E}_h$, we obtain that $v_h = 0$ on Ω. This completes the proof. □

With the above preparations, we state the nonconforming immersed virtual element method as follows: Find $u_h \in V_h(\Omega)$ such that

$$a_h(u_h, v_h) = \langle f, v_h \rangle, \quad \forall v_h \in V_h(\Omega), \tag{3.4}$$

where the loading term $\langle f, \cdot \rangle$ is given by $\langle f, v_h \rangle := (f, \Pi^\nabla v_h)_{0,\Omega}$. Note that the well-posedness of the discrete problem (3.4) follows from Lemma 3.2.

Remark 3.3. The treatment of nonhomogeneous interface conditions is possible using such techniques as in [1, 27]. However, its analysis involves more technical issues. It is left for a future investigation.

4. Approximation properties on interface elements

In this section, we present some approximation properties of the broken linear polynomials and the immersed virtual elements on the interface elements. Note that some estimates were given in [62], but only the special case of the piecewise straight interface was considered. In this paper, we consider the curved interface. From now on, for $X, Y \geq 0$, we write $X \lesssim Y$ or $X \gtrsim Y$ if there exists a constant C depending only on ρ, β and Γ (but independent of the location of the interface intersected with the mesh elements), and $X \eqsim Y$ if both $X \lesssim Y$ and $Y \lesssim X$ hold.

4.1. Some technical inequalities.

We present some technical inequalities used in the analysis of our scheme. We first recall the Poincaré-Friedrichs inequality and the trace inequality (see [18, Section 2]): For any $K \in \mathcal{P}_h$,

$$h_K^{-1} \|v\|_{0,K} \lesssim h_K^{-1} \left| \int_{\partial K} v \, \mathrm{d}s \right| + |v|_{1,K}, \quad \forall v \in H^1(K), \tag{4.1}$$

$$\|v\|_{0,\partial K}^2 \lesssim h_K^{-1} \|v\|_{0,K}^2 + h_K |v|_{1,K}^2, \quad \forall v \in H^1(K). \tag{4.2}$$

Next, for $\delta > 0$, let

$$\Omega_\Gamma^\delta := \{ \boldsymbol{x} \in \Omega : \operatorname{dist}(\boldsymbol{x}, \Gamma) < \delta \},$$

where $\operatorname{dist}(\boldsymbol{x}, \Gamma)$ denotes the distance between $\boldsymbol{x}$ and Γ. Since Γ is C^2, there exists $\delta_0 > 0$ such that the signed distance function ρ, which is defined by

$$\rho(\boldsymbol{x}) := \begin{cases} \operatorname{dist}(\boldsymbol{x}, \Gamma) & \text{if } \boldsymbol{x} \in \Omega^+ \cap \Omega_\Gamma^{\delta_0}, \\ -\operatorname{dist}(\boldsymbol{x}, \Gamma) & \text{if } \boldsymbol{x} \in \Omega^- \cap \Omega_\Gamma^{\delta_0}, \\ 0 & \text{if } \boldsymbol{x} \in \Gamma, \end{cases}$$

is a C^2-function on $\Omega_\Gamma^{\delta_0}$ such that $\|\rho\|_{W^{2,\infty}(\Omega_\Gamma^{\delta_0})} \lesssim 1$ (see [37, 45]). Moreover, since $|\nabla \rho| = 1$ on $\Omega_\Gamma^{\delta_0}$, the unit normal and tangential vectors $\boldsymbol{n}_\Gamma$ and $\boldsymbol{t}_\Gamma$ along Γ can be extended to the region $\Omega_\Gamma^{\delta_0}$ as follows:

$$\boldsymbol{n}_\Gamma = \nabla \rho, \quad \boldsymbol{t}_\Gamma = \left(\frac{\partial \rho}{\partial x_2}, -\frac{\partial \rho}{\partial x_1} \right).$$

Thus $\boldsymbol{n}_\Gamma$ and $\boldsymbol{t}_\Gamma$ can be regarded as $C^1(\Omega_\Gamma^{\delta_0})$-functions such that

$$\|\boldsymbol{n}_\Gamma\|_{W^{1,\infty}(\Omega_\Gamma^{\delta_0})} \lesssim 1, \quad \|\boldsymbol{t}_\Gamma\|_{W^{1,\infty}(\Omega_\Gamma^{\delta_0})} \lesssim 1. \tag{4.3}$$

Note that for sufficiently small h (more precisely, for $h < \delta_0$), any interface element in $\mathcal{P}_h^I$ is included in $\Omega_\Gamma^{\delta_0}$.

Next, let $K \in \mathcal{P}_h^I$. Note that both $\boldsymbol{n}_\Gamma^h$ and $\boldsymbol{t}_\Gamma^h$ are constant on Γ_h^K, and thus can be regarded as constant vector fields on K. Since Γ is C^2, for sufficiently small h, there exist an interval I_K with $|I_K| \lesssim h_K$, a $C^2(I_K)$-function γ_K and $\boldsymbol{x}_0 \in \Gamma_h^K$ such that the following mappings are parametrizations of $\Gamma \cap K$ and Γ_h^K, respectively:

$$s \mapsto \boldsymbol{x}_0 + s\boldsymbol{t}_\Gamma^h + \gamma_K(s)\boldsymbol{n}_\Gamma^h, \quad s \mapsto \boldsymbol{x}_0 + s\boldsymbol{t}_\Gamma^h. \tag{4.4}$$

Since Γ_h^K is the line segment connecting the intersections of Γ and ∂K,

$$\|\gamma_K\|_{W^{m,\infty}(I_K)} \lesssim h_K^{2-m}, \quad m = 0, 1, 2. \tag{4.5}$$

Using (4.3), (4.4) and (4.5) we obtain

$$\|\boldsymbol{n}_\Gamma - \boldsymbol{n}_\Gamma^h\|_{L^\infty(\overline{K})} \lesssim h_K, \quad \|\boldsymbol{t}_\Gamma - \boldsymbol{t}_\Gamma^h\|_{L^\infty(\overline{K})} \lesssim h_K. \tag{4.6}$$

By the definition of β_h, we have

$$\beta|_e = \beta_h|_e, \quad \forall e \subset \partial K, \qquad \beta = \beta_h \text{ on } K^s \cap K_h^s, \quad s = \pm. \tag{4.7}$$

Finally, we also need some estimates on the sets

$$K_r = K - (K^+ \cap K_h^+) - (K^- \cap K_h^-) \quad \forall K \in \mathcal{P}_h^I, \qquad \Omega_r := \bigcup_{K \in \mathcal{P}_h^I} K_r.$$

That is, K_r is the region bounded by $\Gamma \cap K$ and Γ_h^K, and Ω_r is the region bounded by Γ and Γ_h. By (4.5), there exists $\epsilon > 0$ such that $\epsilon \lesssim h^2$ and $\Gamma_h^K \subset \Omega_\Gamma^\epsilon$. Thus

$$K_r \subset \Omega_\Gamma^\epsilon \cap K, \quad K \in \mathcal{P}_h^I. \tag{4.8}$$

According to [55, Lemma 2.1], the following estimate holds:

$$\|v\|_{0,\Omega_\Gamma^\epsilon} \lesssim h\|v\|_{1,\Omega} \quad \forall v \in H^1(\Omega). \tag{4.9}$$

Let $u \in \widetilde{H}_\Gamma^2(\Omega)$. Then the Sobolev extension theorem (see, e.g., [17, 30]) implies that for each $s = \pm$ there exists $\boldsymbol{v}^s \in (H^1(\Omega))^2$ such that $\boldsymbol{v}^s = \nabla u$ on Ω^s and $\|\boldsymbol{v}^s\|_{1,\Omega} \lesssim \|u\|_{2,\Omega^s}$. Now using (4.9), we obtain

$$\|\nabla u\|_{0,\Omega_\Gamma^\epsilon} \lesssim \|\boldsymbol{v}^+\|_{0,\Omega_\Gamma^\epsilon} + \|\boldsymbol{v}^-\|_{0,\Omega_\Gamma^\epsilon} \lesssim h(\|\boldsymbol{v}^+\|_{1,\Omega} + \|\boldsymbol{v}^-\|_{1,\Omega}) \lesssim h\|u\|_{2,\Omega^\pm}.$$

Combining the estimate above and (4.8), we obtain

$$\|\nabla u\|_{0,\Omega_r} \lesssim \|\nabla u\|_{0,\Omega_\Gamma^\epsilon} \lesssim h\|u\|_{2,\Omega^\pm}. \tag{4.10}$$

4.2. **Approximation by broken linear polynomials.** We consider the approximation properties of the broken linear polynomial space $\widehat{\mathbb{P}}_1(K)$. The following lemma can be seen as a generalization of Bramble-Hilbert lemma (see, e.g., [17, Lemma 4.3.8]) to the space $\widehat{\mathbb{P}}_1(K)$.

Lemma 4.1. *Let $K \in \mathcal{P}_h^I$. For each $u \in \widetilde{H}_\Gamma^2(K)$, there exists $q \in \widehat{\mathbb{P}}_1(K)$ such that*

$$\begin{aligned} &\|u - q\|_{0,K} + h_K|u - q|_{1,K} + h_K\|\beta\nabla u - \beta_h\nabla q\|_{0,K} \\ &\lesssim (h_K\|\nabla u\|_{0,K_r} + h_K^2\|u\|_{2,K^\pm}). \end{aligned} \tag{4.11}$$

Proof. Note that we can decompose ∇u as follows:

$$\nabla u = (\nabla u \cdot \boldsymbol{t}_\Gamma)\boldsymbol{t}_\Gamma + (\nabla u \cdot \boldsymbol{n}_\Gamma)\boldsymbol{n}_\Gamma. \tag{4.12}$$

Since $u \in \widetilde{H}_\Gamma^2(K)$, we have $[\nabla u \cdot \boldsymbol{t}_\Gamma]_{\Gamma\cap K} = 0$ and $[\beta\nabla u \cdot \boldsymbol{n}_\Gamma]_{\Gamma\cap K} = 0$. Thus

$$\nabla u \cdot \boldsymbol{t}_\Gamma \in H^1(K), \quad \beta\nabla u \cdot \boldsymbol{n}_\Gamma \in H^1(K). \tag{4.13}$$

Moreover, it follows from (4.3) that

$$\begin{aligned} |\nabla u \cdot \boldsymbol{t}_\Gamma|_{1,K} &\lesssim |\nabla u \cdot \boldsymbol{t}_\Gamma|_{1,K^+} + |\nabla u \cdot \boldsymbol{t}_\Gamma|_{1,K^-} \\ &\lesssim \sum_{s=\pm} |u|_{2,K^s}\|\boldsymbol{t}_\Gamma\|_{L^\infty(K^s)} + |u|_{1,K^s}\|\boldsymbol{t}_\Gamma\|_{W^{1,\infty}(K^s)} \lesssim \|u\|_{2,K}, \end{aligned} \tag{4.14}$$

and similarly

$$|\beta\nabla u \cdot \boldsymbol{n}_\Gamma|_{1,K} \lesssim \|u\|_{2,K}. \tag{4.15}$$

Let $c_t := (\nabla u \cdot \boldsymbol{t}_\Gamma)_K$ and $c_n := (\beta \nabla u \cdot \boldsymbol{n}_\Gamma)_K$. Then, using (4.1), (4.14) and (4.15),

$$\|\nabla u \cdot \boldsymbol{t}_\Gamma - c_t\|_{0,K} \lesssim h_K |\nabla u \cdot \boldsymbol{t}_\Gamma|_{1,K} \lesssim h_K \|u\|_{2,K^\pm}, \tag{4.16}$$

$$\|\beta \nabla u \cdot \boldsymbol{n}_\Gamma - c_n\|_{0,K} \lesssim h_K |\beta \nabla u \cdot \boldsymbol{n}_\Gamma|_{1,K} \lesssim h_K \|u\|_{2,K^\pm}. \tag{4.17}$$

Now we define $q \in \widehat{\mathbb{P}}_1(T)$ by

$$q = q_0 + (u - q_0)_K \quad \text{where } q_0 = c_t(\boldsymbol{x} \cdot \boldsymbol{t}_\Gamma^h) + \beta_h^{-1} c_n (\boldsymbol{x} \cdot \boldsymbol{n}_\Gamma^h).$$

Then we have $\nabla q = c_t \boldsymbol{t}_\Gamma^h + \beta_h^{-1} c_n \boldsymbol{n}_\Gamma^h$ and

$$\begin{aligned}\|\beta \nabla u - \beta_h \nabla q\|_{0,K} &\le \|\beta(\nabla u \cdot \boldsymbol{t}_\Gamma)\boldsymbol{t}_\Gamma - \beta_h c_t \boldsymbol{t}_\Gamma^h\|_{0,K} + \|\beta(\nabla u \cdot \boldsymbol{n}_\Gamma)\boldsymbol{n}_\Gamma - c_n \boldsymbol{n}_\Gamma^h\|_{0,K} \\ &=: I_1 + I_2.\end{aligned}$$

For I_2, it follows from (4.6), (4.15) and (4.17) that

$$I_2 \le \|(\beta \nabla u \cdot \boldsymbol{n}_\Gamma)(\boldsymbol{n}_\Gamma - \boldsymbol{n}_\Gamma^h)\|_{0,K} + \|\beta \nabla u \cdot \boldsymbol{n}_\Gamma - c_n\|_{0,K} \lesssim h_K \|u\|_{2,K^\pm}.$$

For I_1, using (4.6), (4.14) and (4.16) we obtain

$$\begin{aligned}I_1 &\le \|(\beta - \beta_h)\nabla u\|_{0,K} + \beta^* \|(\nabla u \cdot \boldsymbol{t}_\Gamma)(\boldsymbol{t}_\Gamma - \boldsymbol{t}_\Gamma^h)\|_{0,K} + \beta^* \|\nabla u \cdot \boldsymbol{t}_\Gamma - c_t\|_{0,K} \\ &\lesssim \|(\beta - \beta_h)\nabla u\|_{0,K} + h_K \|u\|_{2,K^\pm}.\end{aligned}$$

For the term $\|(\beta - \beta_h)\nabla u\|_{0,K}$, it follows from (4.7) that

$$\|(\beta - \beta_h)\nabla u\|_{0,K} \lesssim \|\nabla u\|_{0,K_r}. \tag{4.18}$$

Thus we have $I_1 \lesssim \|\nabla u\|_{0,K_r} + C h_K \|u\|_{2,K^\pm}$. Combining the estimates for I_1 and I_2, we obtain

$$\|\beta \nabla u - \beta_h \nabla q\|_{0,K} \lesssim \|\nabla u\|_{0,K_r} + h_K \|u\|_{2,K^\pm}.$$

Next, using (4.18) again we have

$$\begin{aligned}|u - q|_{1,K} &\lesssim \|(\beta_h - \beta)\nabla u\|_{0,K} + \|\beta \nabla u - \beta_h \nabla q\|_{0,K} \\ &\lesssim \|\nabla u\|_{0,K_r} + h_K \|u\|_{2,K^\pm}.\end{aligned}$$

Finally, by (4.1), we have

$$\|u - q\|_{0,K} \lesssim h_K |u - q|_{1,K} \lesssim h_K \|\nabla u\|_{0,K_r} + h_K^2 \|u\|_{2,K^\pm}.$$

This completes the proof of the lemma. □

Using this lemma, we obtain the following projection error estimate.

Lemma 4.2. *Let $K \in \mathcal{P}_h^I$, $u \in \widetilde{H}_\Gamma^2(K)$, and $u_\pi := \Pi_K^\nabla u$. Then we have*

$$\begin{aligned}&\|u - u_\pi\|_{0,K} + h_K |u - u_\pi|_{1,K} + h_K \|\beta \nabla u - \beta_h \nabla u_\pi\|_{0,K} \\ &\quad \lesssim h_K \|\nabla u\|_{0,K_r} + h_K^2 \|u\|_{2,K^\pm}.\end{aligned} \tag{4.19}$$

Proof. Let $q \in \widehat{\mathbb{P}}_1(K)$ satisfy (4.11). By the definition of Π_K^∇,

$$\begin{aligned}\beta_* |u - u_\pi|_{1,K}^2 &\le (\beta_h \nabla(u - u_\pi), \nabla(u - u_\pi))_{0,K} = (\beta_h \nabla(u - u_\pi), \nabla u)_{0,K} \\ &= (\beta_h \nabla(u - u_\pi), \nabla(u - q))_{0,K} \le \beta^* |u - u_\pi|_{1,K} |u - q|_{1,K} \\ &\lesssim |u - u_\pi|_{1,K} (\|\nabla u\|_{0,K_r} + h_K \|u\|_{2,K^\pm}).\end{aligned}$$

Thus we have

$$|u - u_\pi|_{1,K} \lesssim \|\nabla u\|_{0,K_r} + h_K \|u\|_{2,K^\pm}. \tag{4.20}$$

Next, by (3.3), (4.1), and (4.20),

$$\|u - u_\pi\|_{0,K} \lesssim h_K |u - u_\pi|_{1,K} \lesssim h_K \|\nabla u\|_{0,K_r} + h_K^2 \|u\|_{2,K^\pm}.$$

Finally, from (4.20) and (4.18),

$$\|\beta\nabla u - \beta_h\nabla u_\pi\|_{0,K} \lesssim \|\nabla u\|_{0,K_r} + h_K\|u\|_{2,K^\pm}.$$

This completes the proof of the lemma. □

Lemma 4.3. *Let $K \in \mathcal{P}_h^I$, $u \in \widetilde{H}_\Gamma^2(K)$, and $u_\pi := \Pi_K^\nabla u$. Then we have*

$$\|\beta\nabla u - \beta_h\nabla u_\pi\|_{0,\partial K} \lesssim h_K^{-1/2}\|\nabla u\|_{0,K_r} + h_K^{1/2}\|u\|_{2,K^\pm}. \tag{4.21}$$

Proof. As in the proof of Lemma 4.1, we have

$$\begin{aligned}\|\beta\nabla u - \beta_h\nabla u_\pi\|_{0,\partial K} &\le \|(\beta\nabla u\cdot\boldsymbol{t}_\Gamma)\boldsymbol{t}_\Gamma - (\beta_h\nabla u_\pi\cdot\boldsymbol{t}_\Gamma^h)\boldsymbol{t}_\Gamma^h\|_{0,\partial K}\\ &\quad + \|(\beta\nabla u\cdot\boldsymbol{n}_\Gamma)\boldsymbol{n}_\Gamma - (\beta_h\nabla u_\pi\cdot\boldsymbol{n}_\Gamma^h)\boldsymbol{n}_\Gamma^h\|_{0,\partial K}\\ &=: I_1 + I_2.\end{aligned}$$

Using (4.6), (4.7), $\nabla u\cdot\boldsymbol{t}_\Gamma \in H^1(K)$, $\nabla u_\pi\cdot\boldsymbol{t}_\Gamma^h \in H^1(K)$, (4.2) and (4.14), we obtain

$$\begin{aligned}I_1 &\lesssim \big(\|\boldsymbol{t}_\Gamma - \boldsymbol{t}_\Gamma^h\|_{L^\infty(\partial K)} + \|\beta-\beta_h\|_{L^\infty(\partial K)}\big)\|\nabla u\cdot\boldsymbol{t}_\Gamma\|_{0,\partial K}\\ &\quad + \|\nabla u\cdot\boldsymbol{t}_\Gamma - \nabla u_\pi\cdot\boldsymbol{t}_\Gamma^h\|_{0,\partial K}\\ &\lesssim h_K\|\nabla u\cdot\boldsymbol{t}_\Gamma\|_{0,\partial K} + \|\nabla u\cdot\boldsymbol{t}_\Gamma - \nabla u_\pi\cdot\boldsymbol{t}_\Gamma^h\|_{0,\partial K}\\ &\lesssim h_K^{1/2}\big(\|\nabla u\cdot\boldsymbol{t}_\Gamma\|_{0,K} + h_K|\nabla u\cdot\boldsymbol{t}_\Gamma|_{1,K}\big)\\ &\quad + h_K^{-1/2}\big(\|\nabla u\cdot\boldsymbol{t}_\Gamma - \nabla u_\pi\cdot\boldsymbol{t}_\Gamma^h\|_{0,K} + h_K|\nabla u\cdot\boldsymbol{t}_\Gamma - \nabla u_\pi\cdot\boldsymbol{t}_\Gamma^h|_{1,K}\big)\\ &\lesssim h_K^{-1/2}\|\nabla u\|_{0,K_r} + h_K^{1/2}\|u\|_{2,K^\pm}.\end{aligned}$$

By a similar argument, one can also obtain

$$I_2 \lesssim h_K^{-1/2}\|\nabla u\|_{0,K_r} + h_K^{1/2}\|u\|_{2,K^\pm}.$$

Now the conclusion follows from the estimates on I_1 and I_2. □

Remark 4.4. Although it is not used in the following sections, one can prove the following interpolation error estimates: For $K \in \mathcal{P}_h^I$, $u \in \widetilde{H}_\Gamma^2(K)$, and $u_I = I_h^K u$,

$$\begin{aligned}&\|u-u_I\|_{0,K} + h_K|u-u_I|_{1,K} + h_K\|\beta\nabla u - \beta_h\nabla u_I\|_{0,K}\\ &\quad\lesssim h_K\|\nabla u\|_{0,K_r} + h_K^2\|u\|_{2,K^\pm}.\end{aligned}$$

5. Error analysis

In this section, we derive the error estimate in the discrete energy norm for the scheme (3.4). We first compute the consistency error.

Lemma 5.1. *Let $u \in H_0^1(\Omega)\cap\widetilde{H}_\Gamma^2(\Omega)$ be the solution of (2.3). Then we have, for any $v_h \in H_h(\Omega)$,*

$$\begin{aligned}a_h(u,v_h) - \langle f, v_h\rangle &= S_h\left(u-\Pi^\nabla u, v_h - \Pi^\nabla v_h\right) + \left(\beta_h\nabla_h\Pi^\nabla u - \beta\nabla u, \nabla_h\Pi^\nabla v_h\right)_{0,\Omega}\\ &\quad + \sum_{K\in\mathcal{P}_h}\left((\beta\nabla u - \beta_h\nabla\Pi^\nabla u)\cdot\boldsymbol{n}_K, \Pi^\nabla v_h - \Pi^\partial v_h\right)_{0,\partial K}.\end{aligned}$$

Proof. Since $[\beta\nabla u\cdot\boldsymbol{n}_e]_e = 0$ for any interior edge $e \in \mathcal{E}_h$, we have

$$\sum_{K\in\mathcal{P}_h}(\beta\nabla u\cdot\boldsymbol{n}_K, \Pi^\partial v_h)_{0,\partial K} = 0. \tag{5.1}$$

Integrating by parts we obtain

$$\begin{aligned}
&a_h(u,v_h)-\langle f,v_h\rangle\\
&\quad= S_h\left(u-\Pi^\nabla u, v_h-\Pi^\nabla v_h\right)+\left(\beta_h\nabla_h\Pi^\nabla u,\nabla_h\Pi^\nabla v_h\right)_{0,\Omega}-\left(f,\Pi^\nabla v_h\right)_{0,\Omega}\\
&\quad= S_h\left(u-\Pi^\nabla u, v_h-\Pi^\nabla v_h\right)+\left(\beta_h\nabla_h\Pi^\nabla u-\beta\nabla u,\nabla_h\Pi^\nabla v_h\right)_{0,\Omega}\\
&\qquad+\sum_{K\in\mathcal{P}_h}\left(\beta\nabla u\cdot\boldsymbol{n}_K,\Pi^\nabla v_h\right)_{0,\partial K}\\
&\quad= S_h\left(u-\Pi^\nabla u, v_h-\Pi^\nabla v_h\right)+\left(\beta_h\nabla_h\Pi^\nabla u-\beta\nabla u,\nabla_h\Pi^\nabla v_h\right)_{0,\Omega}\\
&\qquad+\sum_{K\in\mathcal{P}_h}\left(\beta\nabla u\cdot\boldsymbol{n}_K,\Pi^\nabla v_h-\Pi^\partial v_h\right)_{0,\partial K},
\end{aligned}\tag{5.2}$$

where the last equality follows from (5.1). Note also that, for any $K\in\mathcal{P}_h$,

$$\begin{aligned}
&(\beta_h\nabla\Pi^\nabla u\cdot\boldsymbol{n}_K,\Pi^\partial v_h-\Pi^\nabla v_h)_{0,\partial K}=(\beta_h\nabla\Pi^\nabla u\cdot\boldsymbol{n}_K,v_h-\Pi^\nabla v_h)_{0,\partial K}\\
&\quad=(\nabla\cdot\beta_h\nabla\Pi^\nabla u,v_h-\Pi^\nabla v_h)_{0,K}+(\beta_h\nabla\Pi^\nabla u,\nabla(v_h-\Pi^\nabla v_h))_{0,K}=0,
\end{aligned}\tag{5.3}$$

where the last equality follows from $\nabla\cdot\beta_h\nabla\Pi^\nabla u=0$, which is a direct consequence of the fact that $\Pi_K^\nabla u\in\widehat{\mathbb{P}}_1(K)$, and the definition of Π^∇. The conclusion follows from (5.2) and (5.3). □

Lemma 5.2. *Suppose that $u\in H_0^1(\Omega)\cap\widetilde{H}_\Gamma^2(\Omega)$ be the solution of (2.3). Then, for any $v_h\in H_h(\Omega)$,*

$$\left|\sum_{K\in\mathcal{P}_h}\left((\beta\nabla u-\beta_h\nabla\Pi^\nabla u)\cdot\boldsymbol{n}_K,\Pi^\nabla v_h-\Pi^\partial v_h\right)_{0,\partial K}\right|\lesssim h\|u\|_{2,\Omega^\pm}|||v_h|||.$$

Proof. Let $K\in\mathcal{P}_h$. Using (4.21) we have

$$\begin{aligned}
&\left((\beta\nabla u-\beta_h\nabla\Pi^\nabla u)\cdot\boldsymbol{n}_K,\Pi^\nabla v_h-\Pi^\partial v_h\right)_{0,\partial K}\\
&\quad\le\|\beta\nabla u-\beta_h\nabla\Pi^\nabla u\|_{0,\partial K}\|\Pi^\nabla v_h-\Pi^\partial v_h\|_{0,\partial K}\\
&\quad\lesssim(h_K^{1/2}\|u\|_{2,K^\pm}+h_K^{-1/2}\|\nabla u\|_{0,K_r})\|\Pi^\nabla v_h-\Pi^\partial v_h\|_{0,\partial K}.
\end{aligned}$$

Let $c:=\frac{1}{|\partial K|}\int_{\partial K}\Pi^\nabla v_h\,\mathrm{d}s$. By (4.2) and (4.1),

$$\begin{aligned}
\|\Pi^\nabla v_h-\Pi^\partial v_h\|_{0,\partial K}&\le\|\Pi^\nabla v_h-\Pi^\partial\Pi^\nabla v_h\|_{0,\partial K}+\|\Pi^\partial(v_h-\Pi^\nabla v_h)\|_{0,\partial K}\\
&\le\|\Pi^\nabla v_h-c\|_{0,\partial K}+\|\Pi^\partial(c-\Pi^\nabla v_h)\|_{0,\partial K}+\|\Pi^\partial(v_h-\Pi^\nabla v_h)\|_{0,\partial K}\\
&\le 2\|\Pi^\nabla v_h-c\|_{0,\partial K}+\|\Pi^\partial(v_h-\Pi^\nabla v_h)\|_{0,\partial K}\\
&\lesssim h_K^{1/2}(|\Pi^\nabla v_h|_{1,K}+h_K^{-1/2}\|\Pi^\partial(v_h-\Pi^\nabla v_h)\|_{0,\partial K})\lesssim h_K^{1/2}|||v_h|||.
\end{aligned}$$

Now the assertion of the lemma follows from the estimates above and (4.10). □

The following lemma shows that the discrete bilinear form $a_h(\cdot,\cdot)$ is continuous on $H_h(\Omega)$ with respect to the H^1-seminorm.

Lemma 5.3. *It holds that*

$$a_h^K(v,v)\lesssim|v|_{1,K}^2\quad\forall v\in H^1(K),\ K\in\mathcal{P}_h.$$

Proof. Let $K \in \mathcal{P}_h$ and $v \in H^1(K)$. From (3.2),

$$\begin{aligned}\beta_* |\Pi_K^\nabla v|_{1,K}^2 &\le (\beta_h \nabla \Pi_K^\nabla v, \nabla \Pi_K^\nabla v)_{0,K} = (\beta_h \nabla \Pi_K^\nabla v, \nabla v)_{0,K} \\ &\le \beta^* |\Pi_K^\nabla v|_{1,K} |v|_{1,K}. \end{aligned} \tag{5.4}$$

By (4.2), (4.1) and (5.4),

$$\begin{aligned} S_h^K(v - \Pi_K^\nabla v, v - \Pi_K^\nabla v) &\lesssim h_K^{-1} \|v - \Pi_K^\nabla v\|_{0,\partial K}^2 \\ &\lesssim (h_K^{-2} \|v - \Pi_K^\nabla v\|_{0,K}^2 + |v - \Pi_K^\nabla v|_{1,K}^2) \lesssim |v|_{1,K}^2. \end{aligned} \tag{5.5}$$

Combining (5.4)-(5.5), the conclusion follows. □

We now present the error analysis in the energy-norm and the broken H^1-norm.

Theorem 5.4. *Let $u \in H_0^1(\Omega) \cap \widetilde{H}_\Gamma^2(\Omega)$ be the solution of (2.3). Let $u_h \in V_h(\Omega)$ be the solution of (3.4). Then*

$$|||u - u_h||| \lesssim h \|u\|_{2,\Omega^\pm}. \tag{5.6}$$

Proof. Let $u_\pi = \Pi^\nabla u$ and $v_h := u - u_h \in H_h(\Omega)$. By Lemma 5.1,

$$\begin{aligned} |||u - u_h|||^2 &= a_h(u - u_h, v_h) = a_h(u, v_h) - \langle f, v_h \rangle \\ &= S_h\left(u - \Pi^\nabla u, v_h - \Pi^\nabla v_h\right) + \left(\beta_h \nabla_h \Pi^\nabla u - \beta \nabla u, \nabla_h \Pi^\nabla v_h\right)_{0,\Omega} \\ &\quad + \sum_{K \in \mathcal{P}_h} \left((\beta \nabla u - \beta_h \nabla \Pi^\nabla u) \cdot \boldsymbol{n}_K, \Pi^\nabla v_h - \Pi^\partial v_h\right)_{0,\partial K} \\ &=: I_1 + I_2 + I_3. \end{aligned}$$

For I_1, it follows from Lemma 5.3, (4.19) and (4.10) that

$$|I_1| \le |u - u_\pi|_{1,h} |||v_h||| \lesssim h \|u\|_{2,\Omega^\pm} |||v_h|||.$$

Next, for I_2, we obtain from (4.19) and (4.10) that

$$|I_2| \le \left(\sum_{K \in \mathcal{P}_h} \|\beta_h \nabla u_\pi - \beta \nabla u\|_{0,K}^2 \right)^{1/2} |||v_h||| \lesssim h \|u\|_{2,\Omega^\pm} |||v_h|||.$$

Finally, we have $|I_3| \lesssim h \|u\|_{2,\Omega^\pm} |||v_h|||$ by Lemma 5.2. Now the conclusion follows by combining the estimates of I_1, I_2, and I_3. □

Remark 5.5. One can also obtain the estimate for $|u - \Pi^\nabla u_h|_{1,h}$. Let $u_\pi = \Pi^\nabla u$. From (4.19), (4.10), and (5.6), we have

$$\begin{aligned} |u - \Pi^\nabla u_h|_{1,h} &\le |u - u_\pi|_{1,h} + |\Pi^\nabla (u - u_h)|_{1,h} \lesssim |u - u_\pi|_{1,h} + |||u - u_h||| \\ &\lesssim h \|u\|_{2,\Omega^\pm}. \end{aligned}$$

We next present the L^2-norm estimate of $u - \Pi^\nabla u_h$.

Theorem 5.6. *Suppose that Ω is convex. Let $u \in H_0^1(\Omega) \cap \widetilde{H}_\Gamma^2(\Omega)$ be the solution of (2.3), and let $u_h \in V_h(\Omega)$ be the solution of (3.4). Then*

$$\|u - \Pi^\nabla u_h\|_{0,\Omega} \lesssim h^2 (\|u\|_{2,\Omega^\pm} + \|f\|_{0,\Omega}),$$

where the hidden constant also depends on C_Ω in (2.4).

Proof. Let $\eta = u - \Pi^\nabla u_h$. Let $\varphi \in H_0^1(\Omega)$ be the solution of the dual problem

$$(\beta\nabla\varphi, \nabla v)_{0,\Omega} = (\eta, v)_{0,\Omega}, \quad \forall v \in H_0^1(\Omega).$$

Then Theorem 2.1 shows that $\varphi \in \widetilde{H}^2_\Gamma(\Omega)$ and

$$\|\varphi\|_{2,\Omega^\pm} \lesssim \|\eta\|_{0,\Omega}. \tag{5.7}$$

Let $\varphi_h \in V_h(\Omega)$ be the solution of the corresponding discrete problem

$$a_h(\varphi_h, v_h) = \langle \eta, v_h \rangle \quad \forall v_h \in V_h(\Omega).$$

Let $u_\pi = \Pi^\nabla u$, $u_I = I_h u$, $\varphi_\pi = \Pi^\nabla \varphi$, and $\varphi_I = I_h\varphi$. Then we have

$$\begin{aligned}
\|u - \Pi^\nabla u_h\|^2_{0,\Omega} &= (u - \Pi^\nabla u_h, u)_{0,\Omega} - (u - \Pi^\nabla u_h, \Pi^\nabla u_h)_{0,\Omega} \\
&= (\beta\nabla\varphi, \nabla u)_{0,\Omega} - a_h(\varphi_h, u_h) = (\beta\nabla u, \nabla\varphi)_{0,\Omega} - a_h(u_h, \varphi_h) \\
&= (\beta\nabla u, \nabla\varphi)_{0,\Omega} - a_h(u_h, \varphi_I) + a_h(u_h, \varphi_I - \varphi_h) \\
&= (\beta\nabla u, \nabla\varphi)_{0,\Omega} - a_h(u_h, \varphi_I) + a_h(u_I, \varphi_I - \varphi_h) - a_h(u_I - u_h, \varphi_I - \varphi_h) \\
&= (f, \varphi - \varphi_\pi)_{0,\Omega} + a_h(\varphi - \varphi_h, u) - a_h(u - u_h, \varphi - \varphi_h) \\
&=: I_1 + I_2 + I_3, \qquad (5.8)
\end{aligned}$$

where we have used the fact that $\Pi^\nabla_K u_I = \Pi^\nabla_K u$, $\Pi^\partial_K u_I = \Pi^\partial_K u$, $\Pi^\nabla_K \varphi_I = \Pi^\nabla_K \varphi$ and $\Pi^\partial_K \varphi_I = \Pi^\partial_K \varphi$. For I_1, it follows from (4.19), and (4.10) that

$$|I_1| \lesssim h^2 \|f\|_{0,\Omega} \|\varphi\|_{2,\Omega^\pm}.$$

Next, for I_3, from (5.6) we have

$$|I_3| \le |||u - u_h||| |||\varphi - \varphi_h||| \lesssim h^2 \|\varphi\|_{2,\Omega^\pm} \|u\|_{2,\Omega^\pm}.$$

For I_2, proceeding as in the proof of Lemma 5.1, we obtain

$$\begin{aligned}
I_2 &= S_h(\varphi - \varphi_\pi, u - u_\pi) + ((\beta_h - \beta)\nabla\varphi, \nabla_h u_\pi)_{0,\Omega} \\
&\quad + \sum_{K\in\mathcal{P}_h} ((\beta\nabla\varphi - \beta_h\nabla\varphi_\pi)\cdot \boldsymbol{n}_K, u_\pi - u)_{0,\partial K} \\
&=: I_{2,1} + I_{2,2} + I_{2,3}.
\end{aligned}$$

Using the Cauchy-Schwarz inequality, Lemma 5.3, (4.19), and (4.10), we have

$$|I_{2,1}| \lesssim |\varphi - \varphi_\pi|_{1,h} |u - u_\pi|_{1,h} \lesssim h^2 \|\varphi\|_{2,\Omega^\pm} \|u\|_{2,\Omega^\pm}.$$

Using (4.7), (4.19), and (4.10), we have

$$\begin{aligned}
|I_{2,2}| &\le |((\beta_h - \beta)\nabla\varphi, \nabla_h(u_\pi - u))_{0,\Omega}| + |((\beta_h - \beta)\nabla\varphi, \nabla u)_{0,\Omega}| \\
&\lesssim \|\nabla\varphi\|_{0,\Omega_r} |u - u_\pi|_{1,h} + \|\nabla\varphi\|_{0,\Omega_r} \|\nabla u\|_{0,\Omega_r} \lesssim h^2 \|\varphi\|_{2,\Omega^\pm} \|u\|_{2,\Omega^\pm}.
\end{aligned}$$

For $I_{2,3}$, it follows from (4.2), (4.1), (4.21), (4.19), and (4.10), we have

$$\begin{aligned}
|I_{2,3}| &\le \sum_{K\in\mathcal{P}_h} \|\beta\nabla\varphi - \beta_h\nabla\varphi_\pi\|_{0,\partial K} \|u - u_\pi\|_{0,\partial K} \\
&\lesssim \sum_{K\in\mathcal{P}_h} \|\beta\nabla\varphi - \beta_h\nabla\varphi_\pi\|_{0,\partial K} \left(h_K^{-1/2} \|u - u_\pi\|_{0,K} + h_K^{1/2} |u - u_\pi|_{1,K} \right) \\
&\lesssim \sum_{K\in\mathcal{P}_h} h_K^{1/2} \|\beta\nabla\varphi - \beta_h\nabla\varphi_\pi\|_{0,\partial K} |u - u_\pi|_{1,K} \lesssim h^2 \|\varphi\|_{2,\Omega^\pm} \|u\|_{2,\Omega^\pm}.
\end{aligned}$$

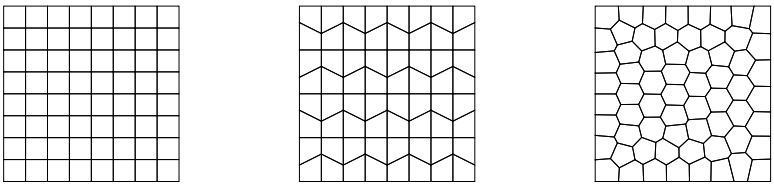

FIGURE 3. The meshes M1 (left), M2 (middle) and M3 (right).

Thus we obtain $|I_2| \lesssim h^2\|\varphi\|_{2,\Omega^\pm}\|u\|_{2,\Omega^\pm}$. Plugging the estimates of I_1, I_2 and I_3 into (5.8), together with (5.7), we obtain

$$\begin{aligned}\|u-\Pi^\nabla u_h\|_{0,\Omega}^2 &\lesssim h^2\|\varphi\|_{2,\Omega^\pm}(\|u\|_{2,\Omega^\pm}+\|f\|_{0,\Omega})\\ &\lesssim h^2(\|u\|_{2,\Omega^\pm}+\|f\|_{0,\Omega})\|u-\Pi^\nabla u_h\|_{0,\Omega}.\end{aligned}$$

This proves the assertion of the theorem. □

6. Numerical tests

In this section, we present some numerical tests for our proposed method.

6.1. **Test case 1: errors and condition number versus h.** We consider the problem (2.1)-(2.2) where $\Omega=(0,1)^2$, and the interface Γ and the subdomains Ω^+ and Ω^- are determined by a given function L:

$$\begin{aligned}\Gamma &= \{(x,y)\in\Omega : L(x,y)=0\},\\ \Omega^+ &= \{(x,y)\in\Omega : L(x,y)>0\},\\ \Omega^- &= \{(x,y)\in\Omega : L(x,y)<0\}.\end{aligned}$$

The level-set function L, the coefficient β and the exact solution u are chosen as in Examples 6.1 to 6.3. We use the following three different families of meshes:

(i) M1: uniform rectangular meshes with $h=1/2^3,1/2^4,\cdots,1/2^7$,
(ii) M2: uniform trapezoidal meshes with $h=1/2^3,1/2^4,\cdots,1/2^7$,
(iii) M3: unstructured polygonal meshes with $h=1/2^3,1/2^4,\cdots,1/2^7$.

Here the meshes in M3 are generated from PolyMesher [63]. Some examples of the meshes are given in Figure 3.

Example 6.1 (straight line interface). In this example, we let

$$\begin{aligned}L(x,y)=2x-y,\quad (\beta^+,\beta^-)=(10^3,1),\\ u(x,y)=1+(x+2y)+(2x-y)/\beta(x,y)+(2x-y)^2,\quad \forall(x,y)\in\Omega.\end{aligned}$$

Example 6.2 (circular interface). Let $r^2=(x-0.5)^2+(y-0.5)^2$ and

$$L(x,y)=r^2-r_0^2,\quad (\beta^+,\beta^-)=(10^4,1),\quad u(x,y)=(r^2-r_0^2)^3/\beta,\quad \forall(x,y)\in\Omega.$$

Example 6.3 (cubic interface). In this example, we let

$$\begin{aligned}L(x,y)=(2y-1)-3(2x-1)(2x-1.3)(2x-1.8)-0.34,\\ (\beta^+,\beta^-)=(10^2,1),\quad u=L/\beta,\quad \forall(x,y)\in\Omega.\end{aligned}$$

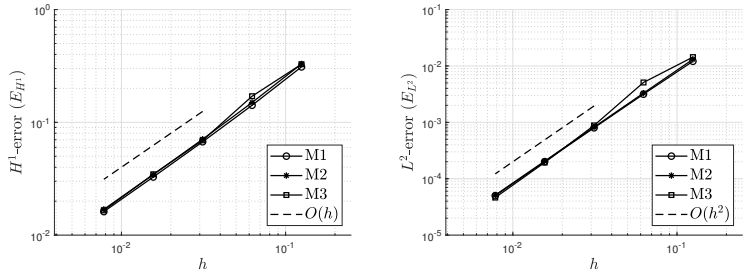

FIGURE 4. Example 6.1: errors versus h of NC-IVEM.

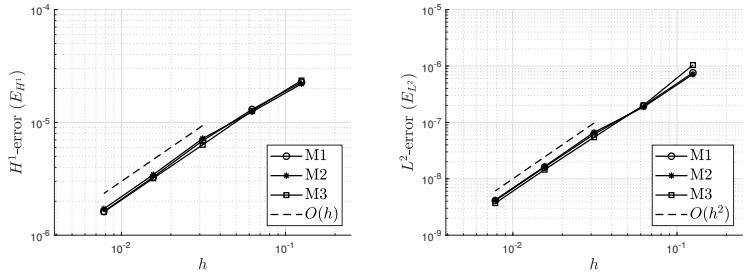

FIGURE 5. Example 6.2: errors versus h of NC-IVEM.

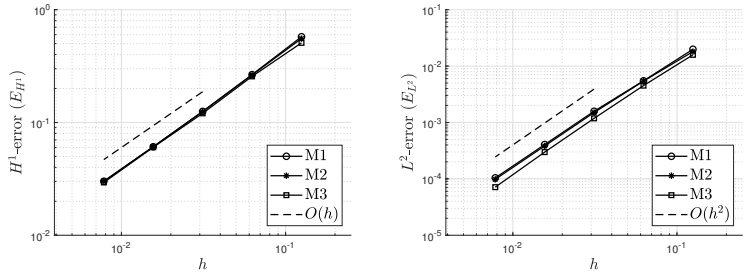

FIGURE 6. Example 6.3: errors versus h of NC-IVEM.

We compute the H^1-seminorm and L^2-norm errors given by

$$E_{H^1} := |u - \Pi^\nabla u_h|_{1,h}, \quad E_{L^2} := \|u - \Pi^\nabla u_h\|_{0,\Omega},$$

where u_h is the solution of our scheme (3.4) (NC-IVEM). For all the examples, we plot the errors versus h in Figures 4 to 6. We observe that the errors converge with optimal order, which is consistent with the theoretical result (see Theorem 5.4, Remark 5.5 and Theorem 5.6). In particular, for Example 6.1, we also plot the results of the immersed WG method (IWG) [62] and the nonconforming immersed FEM (NC-IFEM) [46,52] on the uniform triangular meshes in Figure 7. In contrast with the NC-IVEM, both exhibit suboptimal convergence orders.

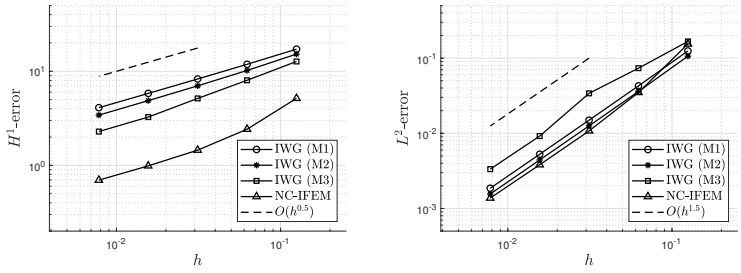

FIGURE 7. Example 6.1: errors versus h of IWG and NC-IFEM.

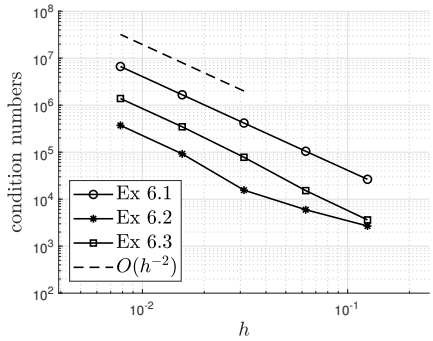

FIGURE 8. Examples 6.1 to 6.3: condition numbers versus h.

Next, we compute the condition number for each example, where the meshes are fixed as M1. We plot the results in Figure 8. We observe that the condition number behaves as usual order $O(h^{-2})$ for all the examples.

6.2. **Test case 2: effect of small-cut edges.** In this test, we investigate the effect of small-cut edges (i.e., the interface edges e with $|e^+| \ll |e^-|$ or $|e^-| \ll |e^+|$) on the condition number and the errors. Consider the problem with $\Omega = (0,1)^2$, $\Gamma = \{(x,y) :\in \Omega : x = 1/2\}$,

$$\Omega^+ = \{(x,y) \in \Omega : x < 1/2\},\ \Omega^- = \{(x,y) \in \Omega : x > 1/2\},$$

and the exact solution u is given by

$$u(x,y) = \begin{cases} 1 + y + (x-1/2)/\beta^+ + (x-1/2)^2 & \text{if } (x,y) \in \Omega^+, \\ 1 + y + (x-1/2)/\beta^- + (x-1/2)^2 & \text{if } (x,y) \in \Omega^-, \end{cases}$$

where $(\beta^+, \beta^-) = (10^2, 1)$ and $(1, 10^2)$. The mesh is built by partitioning Ω into 4×4 squares and relocating the nodes $(1/2, j/4)$ to $(1/2 + \delta, j/4)$ if j is odd and to $(1/2 + 1/8, j/4)$ if j is even, for $\delta = 10^{-3}, 10^{-4}, 10^{-5}, 10^{-6}$ (see Figure 9). In Figures 10 and 11 we plot the condition number and the errors versus δ for each pair (β^+, β^-). Here, the results indicated with the word "mod" will be explained later.

We observe that the condition number seems to be proportional to δ^{-1}. Further theoretical investigation is needed to explain such a phenomenon, which will be a

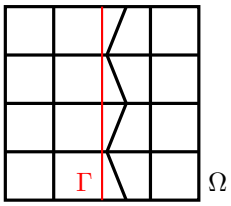

FIGURE 9. Test case 2: the interface (red line) and the mesh (black lines).

subject of future work. In contrast, the errors remain bounded, which is consistent with our theoretical result that the error bounds are independent of the location of the interface intersected with the mesh elements (see Theorem 5.4, Remark 5.5 and Theorem 5.6).

As observed above, the stiffness matrix becomes ill-conditioned in the presence of small-cut edges. However, we can improve the condition number by a simple modification of the discrete interface Γ_h like committing a variational crime in FEM: If e is an interface edge with $|e^-|$ or $|e^+| \lesssim h^2$, then we relocate the intersection point of e and Γ_h to the closest vertex of e, and regard e as a non-interface edge (see Figure 12). This procedure allows us to avoid extremely small-cut edges. The errors of the modified scheme unchanged (see Figure 11 with "mod").

We next compute the condition number of the modified scheme. The results are reported in Figure 10 and are indicated with "mod." We observe that the condition number is uniformly bounded with respect to δ.

6.3. **Test case 3: effect of small-cut cells.** We also investigate the effect of small-cut cells, as in [35]. Consider the problem with $\Omega = (0,1)^2$, $\Omega^- = (0.25, 0.75)^2$, $\Omega^+ = \Omega - \overline{\Omega^-}$, $\Gamma = \partial\Omega^-$ and the exact solution u is given by

$$u(x,y) = \begin{cases} \sin(4\pi x)\sin(4\pi y)/\beta^+ & \text{if } (x,y) \in \Omega^+, \\ \sin(4\pi x)\sin(4\pi y)/\beta^- & \text{if } (x,y) \in \Omega^-, \end{cases}$$

where $(\beta^+, \beta^-) = (10^2, 1)$ and $(1, 10^2)$. The mesh is built by partitioning Ω into 4×4 squares and relocating the nodes $(1/4, j/4)$, $(3/4, j/4)$, $(i/4, 1/4)$ and $(i/4, 3/4)$ to $(1/4+\delta, j/4)$, $(3/4-\delta, j/4)$, $(i/4, 1/4+\delta)$ and $(i/4, 3/4-\delta)$, respectively, for $i, j = 0, 1, \cdots, 4$ and $\delta = 10^{-4}, 10^{-6}, \cdots, 10^{-12}$ (see Figure 13). In Figures 14 and 15 we plot the condition number and the errors versus δ for each pair (β^+, β^-). Similar with the previous numerical test, we observe that the condition number seems to be proportional to δ^{-1}, and the errors remain bounded.

7. Conclusion

We present the lowest-order nonconforming immersed VEM for elliptic interface problems with unfitted polygonal meshes. The local shape functions on the interface elements are defined as solutions of local interface problems with Neumann boundary conditions. We prove that our scheme achieves an optimal convergence rates in the broken H^1-norm and L^2-norm, under the piecewise H^2-regularity assumption. Some numerical tests are carried out to verify the theoretical results.

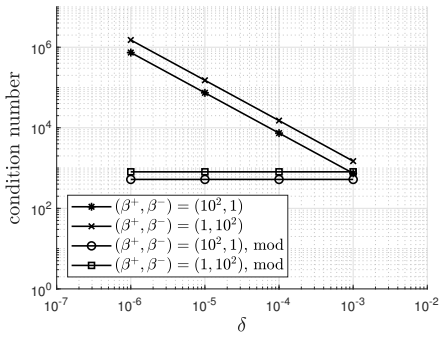

FIGURE 10. Test case 2: the comparison of condition numbers versus δ with and without the discrete interface modification procedure.

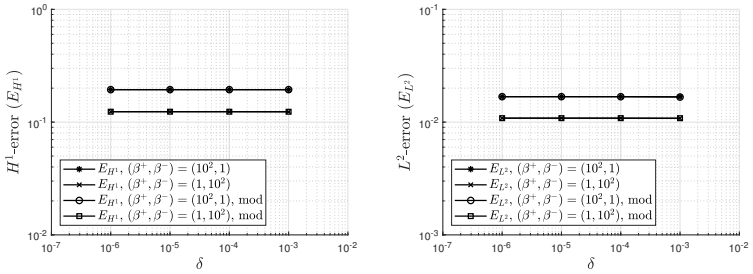

FIGURE 11. Test case 2: the comparison of errors versus δ with and without the discrete interface modification procedure.

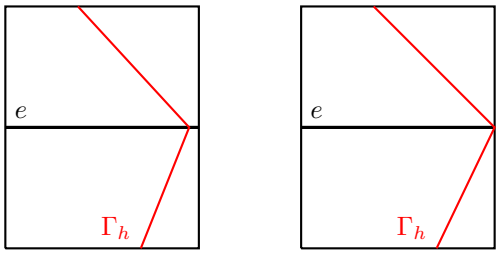

FIGURE 12. The discrete interface Γ_h (red lines) before modification (left) and after modification (right).

REFERENCES

[1] S. ADJERID, I. BABUŠKA, R. GUO, AND T. LIN, *An enriched immersed finite element method for interface problems with nonhomogeneous jump conditions*, Comput. Methods Appl. Mech. Engrg., 404 (2023), pp. Paper No. 115770, 37.

[2] B. AHMAD, A. ALSAEDI, F. BREZZI, L. D. MARINI, AND A. RUSSO, *Equivalent projectors for virtual element methods*, Comput. Math. Appl., 66 (2013), pp. 376–391.

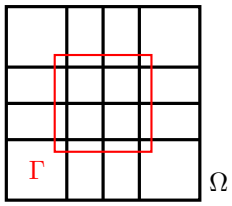

FIGURE 13. Test case 3: the interface (red line) and the mesh (black lines).

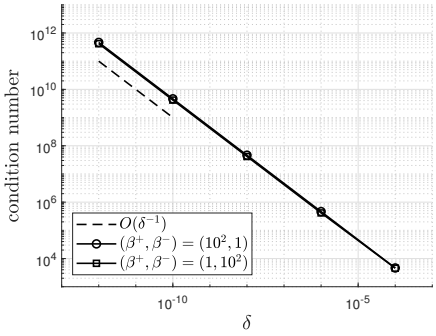

FIGURE 14. Test case 3: the comparison of condition numbers versus δ.

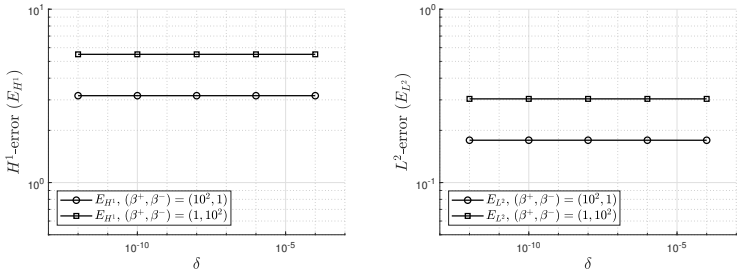

FIGURE 15. Test case 3: the comparison of errors versus δ.

[3] T. ARBOGAST AND Z. CHEN, *On the implementation of mixed methods as nonconforming methods for second-order elliptic problems*, Math. Comp., 64 (1995), pp. 943–972.
[4] D. N. ARNOLD AND F. BREZZI, *Mixed and nonconforming finite element methods: implementation, postprocessing and error estimates*, RAIRO Modél. Math. Anal. Numér., 19 (1985), pp. 7–32.
[5] B. AYUSO DE DIOS, K. LIPNIKOV, AND G. MANZINI, *The nonconforming virtual element method*, ESAIM Math. Model. Numer. Anal., 50 (2016), pp. 879–904.
[6] J. BEAR, *Dynamics of fluids in porous media*, Courier Corporation, 1988.
[7] L. BEIRÃO DA VEIGA, F. BREZZI, A. CANGIANI, G. MANZINI, L. D. MARINI, AND A. RUSSO, *Basic principles of virtual element methods*, Math. Models Methods Appl. Sci., 23 (2013), pp. 199–214.

[8] L. Beirão da Veiga, F. Brezzi, F. Dassi, L. D. Marini, and A. Russo, *A family of three-dimensional virtual elements with applications to magnetostatics*, SIAM J. Numer. Anal., 56 (2018), pp. 2940–2962.
[9] L. Beirão da Veiga, F. Brezzi, and L. D. Marini, *Virtual elements for linear elasticity problems*, SIAM J. Numer. Anal., 51 (2013), pp. 794–812.
[10] L. Beirão da Veiga, F. Brezzi, L. D. Marini, and A. Russo, *The hitchhiker's guide to the virtual element method*, Math. Models Methods Appl. Sci., 24 (2014), pp. 1541–1573.
[11] L. Beirão da Veiga, F. Dassi, G. Manzini, and L. Mascotto, *Virtual elements for Maxwell's equations*, Comput. Math. Appl., 116 (2022), pp. 82–99.
[12] L. Beirão da Veiga, K. Lipnikov, and G. Manzini, *The mimetic finite difference method for elliptic problems*, vol. 11 of MS&A. Modeling, Simulation and Applications, Springer, Cham, 2014.
[13] L. Beirão da Veiga, C. Lovadina, and G. Vacca, *Divergence free virtual elements for the Stokes problem on polygonal meshes*, ESAIM Math. Model. Numer. Anal., 51 (2017), pp. 509–535.
[14] T. Belytschko and T. Black, *Elastic crack growth in finite elements with minimal remeshing*, International journal for numerical methods in engineering, 45 (1999), pp. 601–620.
[15] T. Belytschko, C. Parimi, N. Moës, N. Sukumar, and S. Usui, *Structured extended finite element methods for solids defined by implicit surfaces*, International journal for numerical methods in engineering, 56 (2003), pp. 609–635.
[16] J. H. Bramble and J. T. King, *A finite element method for interface problems in domains with smooth boundaries and interfaces*, Adv. Comput. Math., 6 (1996), pp. 109–138.
[17] S. C. Brenner and L. R. Scott, *The mathematical theory of finite element methods*, vol. 15 of Texts in Applied Mathematics, Springer, New York, third ed., 2008.
[18] S. C. Brenner and L.-Y. Sung, *Virtual element methods on meshes with small edges or faces*, Math. Models Methods Appl. Sci., 28 (2018), pp. 1291–1336.
[19] F. Brezzi, A. Buffa, and K. Lipnikov, *Mimetic finite differences for elliptic problems*, M2AN Math. Model. Numer. Anal., 43 (2009), pp. 277–295.
[20] F. Brezzi, R. S. Falk, and L. D. Marini, *Basic principles of mixed virtual element methods*, ESAIM Math. Model. Numer. Anal., 48 (2014), pp. 1227–1240.
[21] F. Brezzi, K. Lipnikov, and V. Simoncini, *A family of mimetic finite difference methods on polygonal and polyhedral meshes*, Math. Models Methods Appl. Sci., 15 (2005), pp. 1533–1551.
[22] E. Burman, M. Cicuttin, G. Delay, and A. Ern, *An unfitted hybrid high-order method with cell agglomeration for elliptic interface problems*, SIAM J. Sci. Comput., 43 (2021), pp. A859–A882.
[23] E. Burman and A. Ern, *An unfitted hybrid high-order method for elliptic interface problems*, SIAM J. Numer. Anal., 56 (2018), pp. 1525–1546.
[24] A. Cangiani, V. Gyrya, and G. Manzini, *The nonconforming virtual element method for the Stokes equations*, SIAM J. Numer. Anal., 54 (2016), pp. 3411–3435.
[25] S. Cao, L. Chen, and R. Guo, *A virtual finite element method for two-dimensional Maxwell interface problems with a background unfitted mesh*, Math. Models Methods Appl. Sci., 31 (2021), pp. 2907–2936.
[26] S. Cao, L. Chen, R. Guo, and F. Lin, *Immersed virtual element methods for elliptic interface problems in two dimensions*, J. Sci. Comput., 93 (2022), pp. Paper No. 12, 41.
[27] K. S. Chang and D. Y. Kwak, *Discontinuous bubble scheme for elliptic problems with jumps in the solution*, Comput. Methods Appl. Mech. Engrg., 200 (2011), pp. 494–508.
[28] L. Chen, H. Wei, and M. Wen, *An interface-fitted mesh generator and virtual element methods for elliptic interface problems*, J. Comput. Phys., 334 (2017), pp. 327–348.
[29] Z. Chen and J. Zou, *Finite element methods and their convergence for elliptic and parabolic interface problems*, Numer. Math., 79 (1998), pp. 175–202.
[30] P. G. Ciarlet, *The finite element method for elliptic problems*, vol. 40 of Classics in Applied Mathematics, Society for Industrial and Applied Mathematics (SIAM), Philadelphia, PA, 2002. Reprint of the 1978 original [North-Holland, Amsterdam; MR0520174 (58 #25001)].
[31] M. Cicuttin, A. Ern, and N. Pignet, *Hybrid high-order methods—a primer with applications to solid mechanics*, SpringerBriefs in Mathematics, Springer, Cham, [2021] ©2021.

[32] B. Cockburn, D. A. Di Pietro, and A. Ern, *Bridging the hybrid high-order and hybridizable discontinuous Galerkin methods*, ESAIM Math. Model. Numer. Anal., 50 (2016), pp. 635–650.
[33] B. Cockburn, J. Gopalakrishnan, and R. Lazarov, *Unified hybridization of discontinuous Galerkin, mixed, and continuous Galerkin methods for second order elliptic problems*, SIAM J. Numer. Anal., 47 (2009), pp. 1319–1365.
[34] B. Cockburn, J. Guzmán, S.-C. Soon, and H. K. Stolarski, *An analysis of the embedded discontinuous Galerkin method for second-order elliptic problems*, SIAM J. Numer. Anal., 47 (2009), pp. 2686–2707.
[35] F. de Prenter, C. Lehrenfeld, and A. Massing, *A note on the stability parameter in Nitsche's method for unfitted boundary value problems*, Comput. Math. Appl., 75 (2018), pp. 4322–4336.
[36] D. A. Di Pietro and A. Ern, *Hybrid high-order methods for variable-diffusion problems on general meshes*, C. R. Math. Acad. Sci. Paris, 353 (2015), pp. 31–34.
[37] R. L. Foote, *Regularity of the distance function*, Proc. Amer. Math. Soc., 92 (1984), pp. 153–155.
[38] R. Guo and T. Lin, *A higher degree immersed finite element method based on a Cauchy extension for elliptic interface problems*, SIAM J. Numer. Anal., 57 (2019), pp. 1545–1573.
[39] A. Hansbo and P. Hansbo, *An unfitted finite element method, based on Nitsche's method, for elliptic interface problems*, Comput. Methods Appl. Mech. Engrg., 191 (2002), pp. 5537–5552.
[40] ———, *A finite element method for the simulation of strong and weak discontinuities in solid mechanics*, Comput. Methods Appl. Mech. Engrg., 193 (2004), pp. 3523–3540.
[41] X. He, T. Lin, and Y. Lin, *Approximation capability of a bilinear immersed finite element space*, Numer. Methods Partial Differential Equations, 24 (2008), pp. 1265–1300.
[42] T. Y. Hou, Z. Li, S. Osher, and H. Zhao, *A hybrid method for moving interface problems with application to the Hele-Shaw flow*, J. Comput. Phys., 134 (1997), pp. 236–252.
[43] H. Ji, *An immersed Raviart-Thomas mixed finite element method for elliptic interface problems on unfitted meshes*, J. Sci. Comput., 91 (2022), pp. Paper No. 66, 33.
[44] ———, *An immersed Crouzeix-Raviart finite element method in 2D and 3D based on discrete level set functions*, Numer. Math., 153 (2023), pp. 279–325.
[45] H. Ji, F. Wang, J. Chen, and Z. Li, *A new parameter free partially penalized immersed finite element and the optimal convergence analysis*, Numer. Math., 150 (2022), pp. 1035–1086.
[46] ———, *Analysis of nonconforming IFE methods and a new scheme for elliptic interface problems*, ESAIM Math. Model. Numer. Anal., 57 (2023), pp. 2041–2076.
[47] G. Jo and D. Y. Kwak, *An IMPES scheme for a two-phase flow in heterogeneous porous media using a structured grid*, Comput. Methods Appl. Mech. Engrg., 317 (2017), pp. 684–701.
[48] ———, *Geometric multigrid algorithms for elliptic interface problems using structured grids*, Numer. Algorithms, 81 (2019), pp. 211–235.
[49] ———, *Mixed virtual volume methods for elliptic problems*, Comput. Math. Appl., 113 (2022), pp. 345–352.
[50] D. Kwak and J. Lee, *A modified P_1-immersed finite element method*, International Journal of Pure and Applied Mathematics, 104 (2015), pp. 471–494.
[51] D. Y. Kwak and H. Park, *Lowest-order virtual element methods for linear elasticity problems*, Comput. Methods Appl. Mech. Engrg., 390 (2022), pp. Paper No. 114448, 20.
[52] D. Y. Kwak, K. T. Wee, and K. S. Chang, *An analysis of a broken P_1-nonconforming finite element method for interface problems*, SIAM J. Numer. Anal., 48 (2010), pp. 2117–2134.
[53] S. Lee, D. Y. Kwak, and I. Sim, *Immersed finite element method for eigenvalue problem*, J. Comput. Appl. Math., 313 (2017), pp. 410–426.
[54] S. Lemaire, *Bridging the hybrid high-order and virtual element methods*, IMA J. Numer. Anal., 41 (2021), pp. 549–593.
[55] J. Li, J. M. Melenk, B. Wohlmuth, and J. Zou, *Optimal a priori estimates for higher order finite elements for elliptic interface problems*, Appl. Numer. Math., 60 (2010), pp. 19–37.
[56] Z. Li, T. Lin, Y. Lin, and R. C. Rogers, *An immersed finite element space and its approximation capability*, Numer. Methods Partial Differential Equations, 20 (2004), pp. 338–367.

[57] T. Lin, Y. Lin, R. Rogers, and M. L. Ryan, *A rectangular immersed finite element space for interface problems*, in Scientific computing and applications (Kananaskis, AB, 2000), vol. 7 of Adv. Comput. Theory Pract., Nova Sci. Publ., Huntington, NY, 2001, pp. 107–114.
[58] T. Lin, D. Sheen, and X. Zhang, *A nonconforming immersed finite element method for elliptic interface problems*, J. Sci. Comput., 79 (2019), pp. 442–463.
[59] L. Mu, J. Wang, and X. Ye, *A weak Galerkin finite element method with polynomial reduction*, J. Comput. Appl. Math., 285 (2015), pp. 45–58.
[60] L. Mu, J. Wang, X. Ye, and S. Zhao, *A new weak Galerkin finite element method for elliptic interface problems*, J. Comput. Phys., 325 (2016), pp. 157–173.
[61] L. Mu and X. Zhang, *An immersed weak Galerkin method for elliptic interface problems*, J. Comput. Appl. Math., 362 (2019), pp. 471–483.
[62] H. Park and D. Y. Kwak, *An immersed weak Galerkin method for elliptic interface problems on polygonal meshes*, Comput. Math. Appl., 147 (2023), pp. 185–201.
[63] C. Talischi, G. H. Paulino, A. Pereira, and I. F. M. Menezes, `PolyMesher`*: a general-purpose mesh generator for polygonal elements written in Matlab*, Struct. Multidiscip. Optim., 45 (2012), pp. 309–328.
[64] J. Tushar, A. Kumar, and S. Kumar, *Virtual element methods for general linear elliptic interface problems on polygonal meshes with small edges*, Comput. Math. Appl., 122 (2022), pp. 61–75.
[65] J. Wang and X. Ye, *A weak Galerkin mixed finite element method for second order elliptic problems*, Math. Comp., 83 (2014), pp. 2101–2126.
[66] B. Zhang, J. Zhao, Y. Yang, and S. Chen, *The nonconforming virtual element method for elasticity problems*, J. Comput. Phys., 378 (2019), pp. 394–410.

Department of Mathematical Sciences, Korea Advanced Institute of Science and Technology, Daejeon, 34141, Korea
Email address: `hjpark235@kaist.ac.kr`

Department of Mathematical Sciences, Korea Advanced Institute of Science and Technology, Daejeon, 34141, Korea
Email address: `kdy@kaist.ac.kr`